Functional Expansion Tally Capability in the MCS Code

Muhammad Imron [a], Bamidele Ebiwonjumi[a,1], Deokjung Lee [a*],
[a] *Department of Nuclear Engineering, Ulsan National Institute of Science and Technology, 50 UNIST-gil, Ulsan, 44919, Republic of Korea*
[*] *Corresponding author: deokjung@unist.ac.kr*

1. Introduction

The continuous-energy Monte Carlo (MC) is often considered as the most accurate method to solve particle transport problems because it uses fewer approximations compared to deterministic method. For this reason, MC solutions are usually used as reference solutions for deterministic computer codes. Despite this advantage, MC solutions suffer from statistical uncertainties due to the nature of the MC method. Generally, this uncertainty is more severe when one desires localized solutions in which MC tally must be done in very small cells or meshes. This problem could be overcome by increasing number of histories; however, this approach would require expensive computational resources, thus make MC codes less efficient.

In this context, the Functional Expansional Tally (FET) [1,2] can play its role. In FET, the actual solutions are approximated in a truncated linear combination of polynomials and MC tallies are used to determine the corresponding coefficients of the polynomials. Therefore, FET enable to produce continuous representation of tallied quantities in MC simulations. Recently, we have extended MCS capability to produce tally quantities using FET. In this work, we will demonstrate the FET capability in the MCS code [3].

2. Methods

2.1 Functional Expansion Tally

FET solutions are obtained by expanding the tally quantity as a linear combination of polynomials $\psi(\vec{\xi})$ as shown in the Eq. 1

$$f(\vec{\xi}) = \sum_{n=0}^{\infty} \bar{a}_n k_n \psi_n(\vec{\xi}) \quad (1)$$

$$\bar{a}_n = \langle f, \psi_n \rangle = \int_{\Gamma} f(\vec{\xi}) \psi_n(\vec{\xi}) \rho(\vec{\xi}) d\vec{\xi} \quad (2)$$

where $\bar{a}_n$ is the expansion coefficients, $\vec{\xi}$ is the neutron phase space consisting of $(\vec{r}, \vec{\Omega}, \mathrm{E})$, and k_n is the normalization constant which can be calculated according to the choice of the polynomials basis set that is being used

$$k_n = \frac{1}{||\psi_n||^2}$$

and

$$||\psi_n||^2 = \int_{\Gamma} \psi_n^2(\vec{\xi}) \rho(\vec{\xi}) d\vec{\xi} \quad (3)$$

The $\rho(\vec{\xi})$ is the weighting function that shall be both complete and orthogonal with respect to $\psi_n(\vec{\xi})$.

Fortunately, the calculations of the expansion coefficients in Eq. 2 are easily done in MC simulations with both analog and collision-based estimator. The unbiased collision-based estimator for coefficients $\bar{a}_n$ of reaction x is defined in Eq. 4

$$\bar{a}_n = \frac{1}{N} \sum_{i=1}^{N} \sum_{k=1}^{K_i} w_{i,k} \frac{\Sigma_x(\vec{\xi}_{i,k})}{\Sigma_t(\vec{\xi}_{i,k})} \psi_n(\vec{\xi}_{i,k}) \rho(\vec{\xi}_{i,k}) \quad (4)$$

where N is the total number of particles in each batch, K_i is the total number of collisions of particle i, $w_{i,k}$ is the particle i weight at collision k, $\Sigma_x(\vec{\xi}_{i,k})$ is the macroscopic cross section for reaction x at phase space $\vec{\xi}_{i,k}$, and $\Sigma_t(\vec{\xi}_{i,k})$ is the total macroscopic cross section for reaction x at phase space $\vec{\xi}_{i,k}$ [4].

2.2 Choices of the Polynomial Basis

Although any set polynomial basis can be employed, a set of orthogonal polynomials is usually preferred. By setting weighting function ρ as the zeroth order of a set of orthogonal polynomials which is equal to unity, Eq. 3 and Eq. 4 can be simplified. In the MCS code, the Legendre polynomials are used for rectangular geometry problems and Zernike polynomials are used for radial problems. Note that when constructing the polynomials, the variable must be scaled into its domain. For example, the variable Legendre polynomials must be scaled over the interval [-1, 1].

The construction of Legendre polynomials can be done recursively as follow

$$P_n(x) = \frac{(2n-1)xP_{n-1}(x) - (n-1)P_{n-2}(x)}{n}$$

with $P_0 = 1$ and $P_1 = x$. While for the Zernike polynomials, a very efficient recursive method to

[1] Present address: Plasma Science and Fusion Center, Massachusetts Institute of Technology 190 Albany Street, Cambridge, MA.

construct the radial parts of the Zernike polynomials developed in the reference [5] is adopted in the MCS

$$R_m^n(r) = r\left[R_{n-1}^{|m-1|}(r) + R_{n-1}^{m+1}(r)\right] - R_{n-2}^m(r)$$

where the first few order polynomials can be manually determined. To our knowledge, this method is applied into FET for the first time. Once the radial parts are calculated, the Zernike polynomials can be calculated in a usual fashion.

2.3 FET Implementation in MCS

The multi-dimensional FET implementation in MCS assumes that solutions are separable. For example, in the cylindrical geometry, the solution is assumed separable as follow

$$f(r,\theta,z) = g(r,\theta)h(z)$$

This separability is favored to further save computational memory. Numerical experiments have shown that the separable FET appears to give a rough approximation for non-separable distributions and does so for a fraction of the computational cost of the fully coupled solution [2].

One of the limitations of FET is due to the fact the polynomials only good when approximating a smooth distribution, but they can become less effective if they are used to expand functions that contain discontinuities. As suggested in [2], this issue can be solved by employing a piecewise expansion. In a piecewise expansion, a single tally region with known discontinuities is divided into two or more smaller tallies that are expected to have continuous solutions.

3. Results

3.1 Problem

To demonstrate FET capability in MCS, we developed a hypothetical 2×2 three-dimensional lattice problem with pin diameter of 2 cm and 3 cm of pitch as shown in the Fig. 1. In the radial direction, the lattice has three fuel pins (one pin has 3.1% enrichment fuel and the other two have 2.1% enrichment fuel) and one boron absorber pin. The radial boundary conditions (BCs) are reflective. In the axial direction, 2 cm thick of boron absorber is inserted at the axial center of the 3.1% fuel pin. Other 2 cm thick of boron absorbers are also inserted at the 10 cm above axial center of the 2.1% fuel pins. The lattice height spans from -25 cm to 25 cm with vacuum boundary conditions at the axial direction.

3.2 Axial Power Tally

To perform comparisons between conventional tally and FET, three different cases to solve the lattice problem are established as shown in the Table I. All cases used 25 inactive and 150 of active batches. The FET solutions were obtained using 7th order of Legendre polynomials and 11th order of Zernike polynomials in which a total of 102 expansion coefficients (78 Zernike and 24 Legendre expansion coefficients) were stored during simulation.

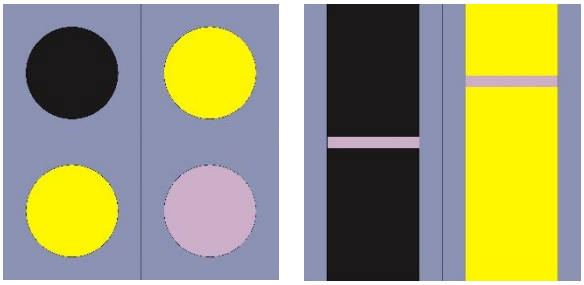

(a) (b)

Fig. 1. (a) Radial and (b) axial views of the lattice problem. Black color denotes 3.1% enrichment fuel, yellow color denotes 2.1% enrichment fuels, pink color denotes boron absorbers, and grey color denotes moderator material.

Table I: Cases to Solve the Lattice Problem

Cases	Tally type	Number histories/ batch
FET	FET	3×10^5
$MESH_{30}$	Conventional mesh tally	3×10^5
$MESH_{200}$	Conventional mesh tally	2×10^6

The axial power tally for the 3.1% enriched fuel pin of the FET case compared to $MESH_{30}$ and $MESH_{200}$ cases are shown in the Fig. 2. To show the FET benefit over conventional mesh tally, the axial power is tallied axially into 10,000 space bins. As shown in the Fig. 2(a), the FET relative axial power is very smooth. In contrast, by using the same number of histories ($MESH_{30}$ case), the conventional mesh tally produces obvious ripples which is a sign of large tally uncertainties. The uncertainties in the $MESH_{30}$ case can be minimized by using higher number histories ($MESH_{200}$ case), which obviously requires more computational resources, and the result compared to FET relative axial power is shown in the Fig. 2(b). The Fig. 2(b) shows improvements in which there are fewer and lower magnitude of the ripples compared to those in Fig. 2(a). The root mean squared (RMS) differences from FET against $MESH_{30}$ and $MESH_{200}$ are 1.6% and 0.9% respectively.

3.3 Radial Power Tally

As for the radial power tally, the particles were sampled into 144,000 space bins (which consist of 40, 72 and 50 meshes in the radial, azimuthal and axial directions respectively) of the 3.1% enriched fuel pin geometry only. The relative radial power of the 3.1% enriched fuel pin at axial position $z = -10$ cm from each case is shown in the Fig. 3.

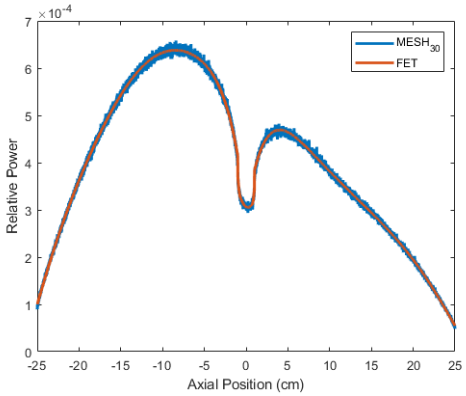

(a)

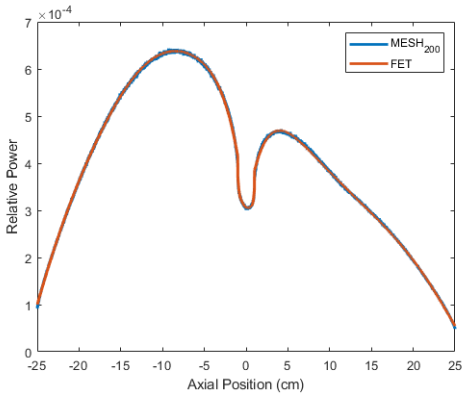

(b)

Fig. 2. FET case relative axial power compared against (a) $MESH_{30}$, and (b) $MESH_{200}$ cases

As shown in the Fig. 3(a), FET can provide a very smooth distribution of the radial power tally. Unlike FET, the traditional mesh tally solutions, with the same number of histories, cannot produce a smooth tally due to large uncertainties. When the number of histories is increased ($MESH_{200}$), the tally distribution is smoother but still showing large uncertainties at the periphery. The RMS difference of the tallied radial power of the FET against $MESH_{30}$ and $MESH_{200}$ are 3.8% and 1.7% respectively.

The running time of FET is slightly lower compared to the conventional mesh tally for the same number of histories because MCS must construct Legendre and/or Zernike polynomials for every collision at given FET regions. However, FET produce a very smooth tally distribution and generally with lower standard deviations (see next section) when the tally must be done in small space bins. When number of histories is increased to achieve smoother distribution ($MESH_{200}$ case), the running time raises by eight folds.

3.4 Standard Deviation

In this section, the standard deviations of the FET will be compared against those from conventional mesh tally. The FET standard deviation calculations require the calculations of the covariance matrix of the individual coefficients' standard deviations. That because their standard deviations are correlated. However, the calculations of covariance matrix during MC simulations are computationally expensive, thus this approach is counterproductive to the objective of the FET. Therefore, only for purpose of this test, we ran an identical problem 30 times in MCS using different random number seeds to calculate the real standard deviations of the tallied quantities. The same lattice problem will be used and the standard deviation for the axial power of the 3.1% enriched fuel pin will be calculated.

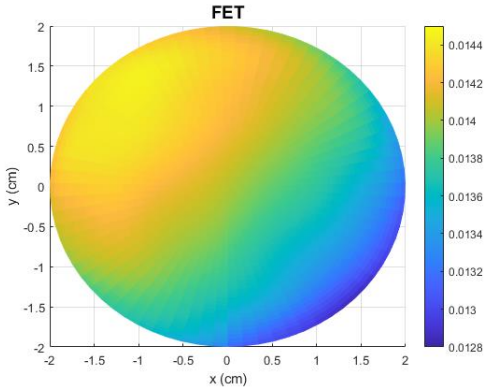

(a)

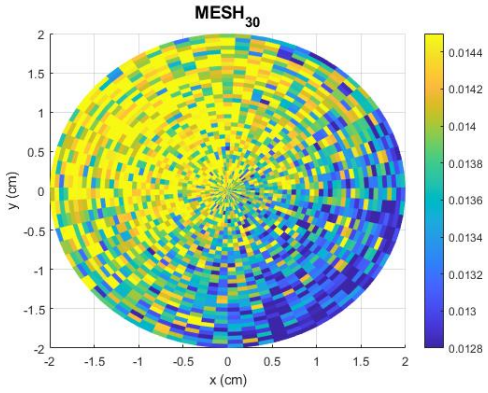

(b)

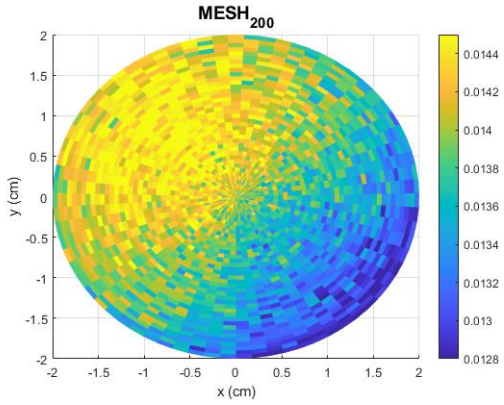

(c)

Fig. 3. Relative radial power tally of the (a) FET, (b) $MESH_{30}$, and (c) $MESH_{200}$ cases

Table II: Running time comparisons

Cases	Running time relative to FET
FET	1
$MESH_{30}$	0.96
$MESH_{200}$	8.34

Table III: Cases to compare standard deviation

Cases	Tally type	Number of axial mesh
FET_{100}	FET	100
FET_{1000}	FET	1000
$MESH_{100}$	Conventional mesh tally	100
$MESH_{1000}$	Conventional mesh tally	1000

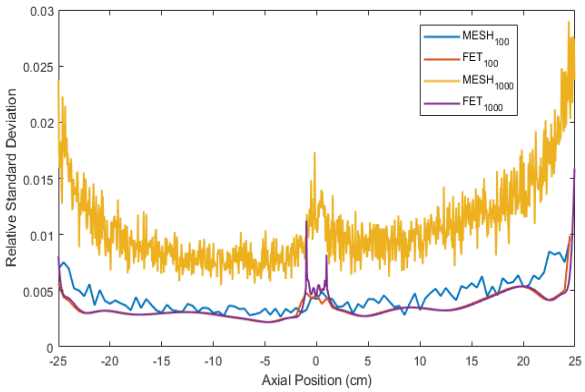

Fig. 4. Axial power tally standard deviations comparisons between FET and conventional mesh tally.

Table III lists four cases to compare the standard deviation from each case. All cases use 25 inactive batches and 150 active batches and 50,000 histories per batch. Fig. 4 clearly shows that FET uncertainties are insensitive to the mesh sizes. Conversely, the conventional mesh tally standard deviation highly depends on the mesh size. The mesh tally standard deviation reduces approximately only by half when the mesh size is increased 10 times. Therefore, if one needs very localized and smooth distribution of the tallied quantities, then FET is preferred over the conventional mesh tally. In this perspective, FET also can be seen as a variance reduction method.

4. Conclusions

FET has been successfully implemented into the MCS code. By using FET, the MCS code can produce a very smooth tallied quantities and generally with lower standard deviation if the tally shall be done in small cells or meshes. Further development to implement FET coupled thermal-hydraulics code to perform reactor multi-physics calculations is underway.

ACKNOWLEDGEMENT

This work was partially supported by the National Research Foundation of Korea (NRF) grant funded by the Korea Government (MSIT). (No. NRF-2019M2D2A1A03058371).

This work was also partially supported by the Korea Institute of Energy Technology Evaluation and Planning and the Ministry of Trade, Industry & Energy (MOTIE) of the Republic of Korea (grant no. 20214000000410).

REFERENCES

[1] W. L. Chadsey, C. W. Wilson, V. W. Pine, W. L. Chadsey, C. W. Wilson, and V. W. Pine, "X-ray photoemission calculations," IEEE Trans. Nucl. Sci., vol. 22, no. 6, pp. 2345–2350, Dec. 1975, doi: 10.1109/TNS.1975.4328131.
[2] D. P. Griesheimer, "Functional Expansion Tallies for Monte Carlo Simulations," PhD thesis, The University of Michigan, 2005.
[3] H. Lee *et al.*, "MCS – A Monte Carlo particle transport code for large-scale power reactor analysis," *Ann. Nucl. Energy*, vol. 139, p. 107276, May 2020.
[4] M. S. Ellis, "Methods for Including Multiphysics Feedback in Monte Carlo Reactor Physics Calculations," PhD thesis, Massachusetts Institute of Technology, 2012.
[5] B. H. Shakibaei and R. Paramesran, "Recursive Formula to Compute Zernike Radial Polynomials," Opt. Lett. Vol. 38, Issue 14, pp. 2487-2489, Jul. 2013.